

Off-forward quark distributions of the nucleon in the large N_c limit

V. Yu. Petrov, P.V. Pobylitsa, M.V. Polyakov¹

Petersburg Nuclear Physics Institute, Gatchina, St.Petersburg 188350, Russia

I. Börnig, K. Goeke, C. Weiss

*Institut für Theoretische Physik II, Ruhr-Universität Bochum,
D-44780 Bochum, Germany*

Abstract

We study the off-forward quark distributions (OFQD's) in the chiral quark-soliton model of the nucleon. This model is based on the large- N_c picture of the nucleon as a soliton of the effective chiral lagrangian and allows to calculate the leading twist quark- and antiquark distributions at a low normalization point. We demonstrate the consistency of the approach by checking various sum rules for the OFQD's. We present numerical estimates of the isosinglet distribution $H(x, \xi, \Delta^2)$. In contrast to other approaches we find a strong qualitative dependence on the longitudinal momentum transfer, ξ . In particular, $H(x, \xi, \Delta^2)$ as a function of x exhibits fast crossovers at $|x| = \xi/2$. Such behaviour could lead to a considerable enhancement of the deeply-virtual Compton scattering cross section.

¹e-mail: maximp@hadron.tp2.ruhr-uni-bochum.de

1 Introduction

Although a large portion of quantitative information about strong interactions is contained in the well-known parton distribution functions of the nucleon, one should not forget that they provide us with still far from complete knowledge of the structure of the nucleon. Recently, a new type of parton distributions has attracted considerable interest, the so called off-forward parton distributions (OFPD's), which are generalizations simultaneously of the usual parton distributions and of the elastic nucleon form factors. Taking the n -th moment of the OFPD's one obtains the form factors (*i.e.*, non-forward matrix elements) of the spin- n , twist-two quark and gluon operators. On the other hand, in the forward limit the OFPD's reduce to the usual quark, antiquark and gluon distributions. In other words, the OFPD's interpolate between the traditional inclusive (parton distributions) and exclusive (form factors) characteristics of the nucleon and thus provide us with a considerable new amount of information on nucleon structure.

The OFPD's are not accessible in standard inclusive measurements. They can, however, be measured in deeply-virtual Compton scattering (DVCS) [1, 2, 3, 6, 7] and in hard exclusive electroproduction of mesons [4, 5, 7]. A firm theoretical basis for the QCD analysis of DVCS and hard exclusive electroproduction of mesons in terms of off-forward parton distributions in the nucleon is provided by the recently proven factorization theorems for these processes [4, 5, 7]. A quantitative description of these classes of processes requires not only knowledge of the perturbative evolution of the OFPD's [3, 4, 7, 8], but also non-perturbative information in the form of the OFPD's at some initial normalization point. Thus, a computation of the OFPD's at a low normalization point in a realistic model of the nucleon is of great importance. While the usual parton distributions have been measured in a variety of different experiments and can be confronted with model calculations *a posteriori*, in the case of the off-forward distributions the situation is rather opposite: Here, model calculations of the distributions at a low normalization point are required to determine the very feasibility of measuring the OFPD's, say, in DVCS at experimental energies.

Recently it was shown that the chiral quark-soliton model of the nucleon [10], which is based on the instanton model of the QCD vacuum, provides a framework for a successful calculation of the nucleon parton distributions, both unpolarized and polarized, at a low normalization point [11, 12, 13, 14]. This is a quantum field-theoretical description of the nucleon, with explicit quark degrees of freedom, which allows an unambiguous identification of the quark as well as antiquark distributions in the nucleon. We were able to demonstrate that all general properties of the quark and antiquark distributions (positivity, sum rules, Soffer inequalities, *etc.*) are correctly realized in this description. At the same time, the chiral quark-soliton model gives a good account of a variety of static properties of the nucleon and other baryons, and of baryon form factors (for a review, see ref. [9]). Given the success in describing both nucleon form factors and the usual parton distribution functions, this approach seems well posed for a theoretical investigation of the off-forward parton distributions of the nucleon at a low normalization point.

Recently, Ji *et al.* have studied the off-forward quark distributions in the bag model [6], providing the first model estimates of these quantities. However, bag models encounter severe problems in applications to parton distribution functions. It is usually assumed

that the three quarks in the bag give rise only to quark distributions; however, they inevitably produce also an antiquark distribution with *negative* sign. This circumstance is not often emphasized. To overcome this problem one would need to add the contribution to the structure function arising from the forces which bind the quarks — in the case of the bag model, from the bag surface. Unfortunately, the latter is not described in terms of fields. In contrast to the bag model our approach ensures the positivity of both quark and antiquark distributions, because the forces which bind the quarks in the nucleon are described consistently in terms of fields. Below we shall see that in the case of off-forward quark distributions (OFQD's) the field-theoretic description leads to characteristic crossovers of the OFQD's at $x = \pm\xi/2$, as opposed to the bag model result, which is smooth at these points.

In this paper we study the off-forward quark and antiquark distributions in the chiral quark–soliton model of the nucleon. In section 2 we outline the QCD definition of the OFPD's and their basic properties. Section 3 gives a brief introduction to the chiral quark soliton model of the nucleon. In section 4 we derive the expressions for the OFQD's in the chiral quark soliton model and show that the sum rules are satisfied within the model. We discuss the contributions to the OFQD's from the bound–state level of quarks as well as from the Dirac continuum, whose presence is a consequence of the field–theoretic character of this description of the nucleon. We show that the latter is crucial near $x = \pm\xi/2$ and lead to sharp crossovers of the OFQD's. Numerical estimates for the singlet unpolarized distribution $H(x, \xi, \Delta^2)$ are presented in section 5. A summary and conclusions are given in section 6.

2 QCD definition of off-forward quark distributions

In QCD the off-forward parton distributions are defined through nondiagonal matrix elements of product of quark fields at light–cone separation. Here and in the following, we shall use the notations of refs. [1, 3]:

$$\begin{aligned} \int \frac{d\lambda}{2\pi} e^{i\lambda x} \langle P' | \bar{\psi}(-\lambda n/2) \not{n} \psi(\lambda n/2) | P \rangle &= H(x, \xi, \Delta^2) \bar{U}(P') \not{n} U(P) \\ &+ \frac{1}{2M_N} E(x, \xi, \Delta^2) \bar{U}(P') i\sigma^{\mu\nu} n_\mu \Delta_\nu U(P). \end{aligned} \tag{2.1}$$

Here n_μ is a light-cone vector,

$$n^2 = 0, \quad n \cdot (P + P') = 2, \tag{2.2}$$

Δ the four–momentum transfer,

$$\Delta = P' - P, \tag{2.3}$$

M_N denotes the nucleon mass, and $U(P)$ is a standard Dirac spinor. The off-forward quark distributions, $H(x, \xi, \Delta^2)$ and $E(x, \xi, \Delta^2)$, are regarded as functions of the variable x , the square of the four–momentum transfer, Δ^2 , and its longitudinal component

$$\xi = -(n \cdot \Delta). \tag{2.4}$$

In the forward case, $P = P'$, both Δ and ξ are zero, and the second term on the r.h.s. of eq.(2.1) disappears. The function H becomes the usual parton distribution function,

$$H(x, \xi = 0, \Delta^2 = 0) = q(x). \quad (2.5)$$

On the other hand, taking the first moment of eq.(2.1) one reduces the operator on the l.h.s. to the local vector current. The dependence of H and E on ξ disappears, and the functions reduce to the usual electric and magnetic form factors of the nucleon,

$$\int_{-1}^1 dx H(x, \xi, \Delta^2) = F_1(\Delta^2), \quad (2.6)$$

$$\int_{-1}^1 dx E(x, \xi, \Delta^2) = F_2(\Delta^2). \quad (2.7)$$

Taking higher moments of the distribution functions one obtains the form factors of the twist-2, spin- n operators.

3 Chiral quark–soliton model of the nucleon

Recently a new approach to the calculation of quark distribution functions has been developed [12] within the context of the chiral quark-soliton model of the nucleon [10]. In this paper we apply this approach to the calculation of OFQD's. It is essentially based on the $1/N_c$ expansion. Although in reality the number of colours $N_c = 3$, the academic limit of large N_c is known to be a useful guideline. At large N_c the nucleon is heavy and can be viewed as a classical soliton of the pion field [15, 16]. In this paper we work with the effective chiral action given by the functional integral over quarks in the background pion field [17, 18, 19]:

$$\exp(iS_{\text{eff}}[\pi(x)]) = \int D\psi D\bar{\psi} \exp\left(i \int d^4x \bar{\psi}(i\rlap{\not{D}} - MU\gamma_5)\psi\right),$$

$$U = \exp[i\pi^a(x)\tau^a], \quad U\gamma_5 = \exp[i\pi^a(x)\tau^a\gamma_5] = \frac{1 + \gamma_5}{2}U + \frac{1 - \gamma_5}{2}U^\dagger. \quad (3.8)$$

Here ψ is the quark field, M the effective quark mass, which is due to the spontaneous breakdown of chiral symmetry (generally speaking, it is momentum dependent), and U is the $SU(2)$ chiral pion field. The effective chiral action given by (3.8) is known to contain automatically the Wess–Zumino term and the four-derivative Gasser–Leutwyler terms, with correct coefficients. Equation (3.8) has been derived from the instanton model of the QCD vacuum [19, 20], which provides a natural mechanism of chiral symmetry breaking and enables one to express the dynamical mass M and the ultraviolet cutoff intrinsic in (3.8) through the Λ_{QCD} parameter. The ultraviolet regularization of the effective theory is provided by the specific momentum dependence of the mass, $M(p^2)$, which drops to zero for momenta of order of the inverse instanton size in the instanton vacuum, $1/\rho \sim 600$ MeV. For simplicity we shall neglect this momentum dependence in the general discussion; it will be taken into account again in the theoretical analysis and in the numerical estimates later.

An immediate application of the effective chiral theory (3.8) is the quark-soliton model of baryons of ref. [10], which is in the spirit of the earlier works [21, 22]. According to this model nucleons can be viewed as N_c “valence” quarks bound by a self-consistent pion field (the “soliton”) whose energy coincides with the aggregate energy of the quarks of the negative-energy Dirac continuum. Similarly to the Skyrme model large N_c is needed as a parameter to justify the use of the mean-field approximation; however, the $1/N_c$ -corrections can be — and, in some cases, have been — computed [9].

Let us remind the reader how the nucleon is described in the effective low-energy theory (3.8). Integrating out the quarks in (3.8) one finds the effective chiral action,

$$S_{\text{eff}}[\pi^a(x)] = -N_c \text{Sp} \log D(U), \quad D(U) = i\partial_0 - H(U), \quad (3.9)$$

where $H(U)$ is the one-particle Dirac hamiltonian,

$$H(U) = -i\gamma^0\gamma^k\partial_k + M\gamma^0U\gamma^5, \quad (3.10)$$

and $\text{Sp} \dots$ denotes the functional trace. For a given time-independent pion field $U = \exp(i\pi^a(\mathbf{x})\tau^a)$ one can determine the spectrum of the Dirac hamiltonian,

$$H\Phi_n = E_n\Phi_n. \quad (3.11)$$

It contains the upper and lower Dirac continua (distorted by the presence of the external pion field), and, in principle, also discrete bound-state level(s), if the pion field is strong enough. If the pion field has unity winding number, there is exactly one bound-state level which travels all the way from the upper to the lower Dirac continuum as one increases the spatial size of the pion field from zero to infinity [10]. We denote the energy of the discrete level as E_{lev} , $-M \leq E_{\text{lev}} \leq M$. One has to occupy this level to get a non-zero baryon number state. Since the pion field is colour blind, one can put N_c quarks on that level in the antisymmetric state in colour.

The limit of large N_c allows us to use the mean-field approximation to find the nucleon mass. To get the nucleon mass one has to add $N_c E_{\text{lev}}$ and the energy of the pion field. Since the effective chiral lagrangian is given by the determinant (3.9) the energy of the pion field coincides exactly with the aggregate energy of the lower Dirac continuum, the free continuum subtracted. The self-consistent pion field is thus found from the minimization of the functional [10]

$$M_N = \min_U N_c \left\{ E_{\text{lev}}[U] + \sum_{E_n < 0} (E_n[U] - E_n^{(0)}) \right\}. \quad (3.12)$$

From symmetry considerations one looks for the minimum in a hedgehog ansatz:

$$U_c(\mathbf{x}) = \exp[i\pi^a(\mathbf{x})\tau^a] = \exp[in^a\tau^a P(r)], \quad r = |\mathbf{x}|, \quad \mathbf{n} = \frac{\mathbf{x}}{r}, \quad (3.13)$$

where $P(r)$ is called the profile of the soliton.

The minimum of the energy (3.12) is degenerate with respect to translations of the soliton in space and to rotations of the soliton field in ordinary and isospin space. For the hedgehog field (3.13) the two rotations are equivalent. The projection on a nucleon

state with given spin (S_3) and isospin (T_3) components is obtained by integrating over all spin-isospin rotations, R [16, 10],

$$\langle S = T, S_3, T_3 | \dots | S = T, S_3, T_3 \rangle = \int dR \phi_{S_3 T_3}^{*S=T}(R) \dots \phi_{S_3 T_3}^{S=T}(R). \quad (3.14)$$

Here $\phi_{S_3 T_3}^{S=T}(R)$ is the rotational wave function of the nucleon given by the Wigner finite-rotation matrix [16, 10]:

$$\phi_{S_3 T_3}^{S=T}(R) = \sqrt{2S+1}(-1)^{T+T_3} D_{-T_3, S_3}^{S=T}(R). \quad (3.15)$$

Analogously, the projection on a nucleon state with given momentum \mathbf{P} is obtained by integrating over all shifts, \mathbf{X} , of the soliton,

$$\langle \mathbf{P}' | \dots | \mathbf{P} \rangle = \int d^3\mathbf{X} e^{i(\mathbf{P}'-\mathbf{P})\cdot\mathbf{X}} \dots \quad (3.16)$$

4 Off-forward quark distributions in the chiral quark-soliton model

We now turn to the calculation of the off-forward quark distributions in the chiral quark-soliton model. This description of the nucleon is based on the $1/N_c$ -expansion. At large N_c the nucleon is heavy — its mass is $O(N_c)$. Thus for the large- N_c nucleon eq. (2.1) simplifies as follows:

$$\begin{aligned} \int \frac{d\lambda}{2\pi} e^{i\lambda x} \langle P', S'_3 | \bar{\psi}(-\lambda n/2) \not{n} \psi(\lambda n/2) | P, S_3 \rangle &= 2\delta_{S'_3 S_3} H(x, \xi, \Delta^2) \\ &- \frac{i}{M_N} \epsilon^{3jk} \Delta^j (\sigma^k)_{S'_3 S_3} E(x, \xi, \Delta^2), \end{aligned} \quad (4.17)$$

where S_3, S'_3 denote the projections of the nucleon spin.

Before computing the quark distribution functions we must determine the parametric order in $1/N_c$ of the kinematical variables involved. Generally, when describing parton distributions in the large- N_c limit, $x \sim 1/N_c$, since the nucleon momentum is distributed among N_c quarks. Furthermore, as in the calculation of nucleon form factors we consider momentum transfers $\Delta^2 \sim N_c^0$; hence, in particular, $\xi \sim 1/N_c$, so that ξ is of the same parametric order as x .

The calculation of the off-forward parton distributions proceeds in much the same way as that of the usual parton distributions [12]. One expands the quark fields in eq.(4.17) in the basis of quark single-particle wave functions in the background pion field, eq.(3.11). The nucleon matrix element is then obtained by summing over all occupied single-particle states (the bound-state level and the negative-energy continuum) and projecting on nucleon states with definite spin and momenta by integrating over collective coordinates of the soliton field with appropriate wave functions, *cf.* eqs.(3.14, 3.16). When integrating over soliton rotations one must consider separately flavour singlet and nonsinglet matrix elements. In the flavour singlet case the integral over soliton rotations is trivial, and one

obtains

$$\begin{aligned}
& \int \frac{d\lambda}{2\pi} e^{i\lambda x} \sum_f \langle P', T' = S', T'_3, S'_3 | \bar{\psi}_f(-\lambda n/2) \not{\eta} \psi_f(\lambda n/2) | P, T = S, T_3, S_3 \rangle \\
&= \frac{N_c M_N^2}{\pi} \delta_{TT'} \delta_{SS'} \delta_{T_3 T'_3} \delta_{S_3 S'_3} \int dz^0 \int d^3 \mathbf{X} \exp[i\boldsymbol{\Delta} \cdot \mathbf{X}] \\
&\quad \times \sum_{\text{occup.}} \exp\{iz^0[(x + \xi/2)M_N - E_n]\} \Phi_n^\dagger(\mathbf{X}) \gamma^0 \not{\eta} \Phi_n(\mathbf{X} - z^0 \mathbf{e}_3), \quad (4.18)
\end{aligned}$$

where \mathbf{e}_3 is the unit vector in the third direction. This equation was derived in [12] for the case $P' = P$; the generalization to $P' \neq P$ is straightforward. [Here and in the analogous expressions below it is understood that one subtracts the sums over levels of the vacuum hamiltonian ($U = 1$).] For the flavour nonsinglet part, on the other hand, one has

$$\begin{aligned}
& \int \frac{d\lambda}{2\pi} e^{i\lambda x} \langle P', T' = S', T'_3, S'_3 | \bar{\psi}(-\lambda n/2) \tau^a \not{\eta} \psi(\lambda n/2) | P, T = S, T_3, S_3 \rangle \\
&= \frac{N_c M_N^2}{\pi} \int dz^0 \int d^3 \mathbf{X} \exp[i\boldsymbol{\Delta} \cdot \mathbf{X}] \int dR \phi_{T'_3 S'_3}^{T'=S'^*}(R) \phi_{T_3 S_3}^{T=S}(R) \frac{1}{2} \text{Tr}(R^\dagger \tau^a R \tau^b) \\
&\quad \times \sum_{\text{occup.}} \exp\{iz^0[(x + \xi/2)M_N - E_n]\} \Phi_n^\dagger(\mathbf{X}) \tau^b \gamma^0 \not{\eta} \Phi_n(\mathbf{X} - z^0 \mathbf{e}_3). \quad (4.19)
\end{aligned}$$

Here $\phi_{T'_3 S'_3}^{T=S}(R)$ are the rotational wave functions of the soliton, eq.(3.15). The integral over the soliton orientation matrix R can be computed,

$$\int dR \phi_{T'_3 S'_3}^{\frac{1}{2}*}(R) \phi_{T_3 S_3}^{\frac{1}{2}}(R) \frac{1}{2} \text{Tr}(R^\dagger \tau^a R \tau^b) = -\frac{1}{3} (\tau^a)_{T'_3 T_3} (\sigma^b)_{S'_3 S_3}. \quad (4.20)$$

Comparing eq.(4.18) and eqs.(4.19, 4.20) with eq.(4.17) we immediately see that in the leading order of the $1/N_c$ expansion only the flavour singlet part of $H(x, \xi, \Delta^2)$ and the flavour-nonsinglet part of $E(x, \xi, \Delta^2)$ are non-zero. They are given, respectively, by

$$\begin{aligned}
\sum_f H_f(x, \xi, \Delta^2) &= \frac{N_c M_N}{2\pi} \int dz^0 \int d^3 \mathbf{X} \exp[i\boldsymbol{\Delta} \cdot \mathbf{X}] \\
&\quad \times \sum_{\text{occup.}} \exp\{iz^0[(x + \xi/2)M_N - E_n]\} \Phi_n^\dagger(\mathbf{X}) (1 + \gamma^0 \gamma^3) \Phi_n(\mathbf{X} - z^0 \mathbf{e}_3), \quad (4.21)
\end{aligned}$$

$$\begin{aligned}
\epsilon^{3jk} \Delta^j E^{(3)}(x, \xi, \Delta^2) &= -\frac{i N_c M_N^2}{3\pi} \int dz^0 \int d^3 \mathbf{X} \exp[i\boldsymbol{\Delta} \cdot \mathbf{X}] \\
&\quad \times \sum_{\text{occup.}} \exp\{iz^0[(x + \xi/2)M_N - E_n]\} \Phi_n^\dagger(\mathbf{X}) \tau^k (1 + \gamma^0 \gamma^3) \Phi_n(\mathbf{X} - z^0 \mathbf{e}_3). \quad (4.22)
\end{aligned}$$

The isovector part of $H(x, \xi, \Delta^2)$ and the isosinglet part of $E(x, \xi, \Delta^2)$ appear only in the next-to-leading order of the $1/N_c$ -expansion, *i.e.*, after taking into account the finite angular velocity of the soliton rotation.

Before going ahead with the evaluation of the expressions eqs.(4.21, 4.22) we would like to demonstrate that the two limiting cases of the off-forward distributions — usual parton distributions and elastic form factors — are correctly reproduced within the chiral quark-soliton model. Taking in eq.(4.21) the forward limit, $\Delta \rightarrow 0$, one recovers the

formula for the usual singlet (anti-) quark distributions in our model which was obtained in ref.[12]. Thus the forward limit, eq.(2.5), is reproduced. On the other hand, integrating eqs.(4.21,4.22) over $-1 \leq x \leq 1$ one obtains (up to corrections parametrically small in $1/N_c$) the expressions for the electromagnetic formfactors of the nucleon derived in ref. [10]:

$$\int_{-1}^1 dx \sum_f H_f(x, \xi, \Delta^2) = N_c \int d^3 \mathbf{X} \exp[i\mathbf{\Delta} \cdot \mathbf{X}] \sum_{\text{occup.}} \Phi_n^\dagger(\mathbf{X}) \Phi_n(\mathbf{X})$$

$$= F_1^{(T=0)}(\Delta^2), \quad (4.23)$$

$$\int_{-1}^1 dx E^{(3)}(x, \xi, \Delta^2) = -\frac{iN_c M_N}{\Delta^2} \varepsilon_{3ik} \Delta^i \int d^3 \mathbf{X} \exp[i\mathbf{\Delta} \cdot \mathbf{X}] \sum_{\text{occup.}} \Phi_n^\dagger(\mathbf{X}) \gamma^0 \gamma^3 \tau^k \Phi_n(\mathbf{X})$$

$$= F_2^{(T=1)}(\Delta^2). \quad (4.24)$$

The electromagnetic formfactors computed in the chiral quark soliton model on the basis of these formulas compare very well with the experimentally measured ones up to momenta of order $\Delta^2 \sim 1 \text{ GeV}^2$ [9, 23].

Eqs. (4.21,4.22) express the OFPD's as a sum over quark single-particle levels in the soliton field. This sum runs over *all* occupied levels, including both the discrete bound-state level and the negative Dirac continuum. We remind the reader that in the case of usual parton distributions it was demonstrated that in order to ensure the positivity of the antiquark distributions it is essential to take into account the contributions of *all* occupied levels of the Dirac Hamiltonian [12]. The so-called ‘‘valence level approximation’’ for structure functions in the chiral quark-soliton model advocated in [24] leads to unacceptable *negative* antiquark distributions. We shall see below that also in the off-forward case the contribution of the Dirac continuum drastically changes the shape of the distribution function, leading to characteristic crossovers of $H(x, \xi, \Delta)$ at $|x| = \xi/2$.

We shall now compute the contributions of the discrete bound-state level and the negative Dirac continuum to eqs. (4.21,4.22). We focus here on the isosinglet distribution $H(x, \xi, \Delta)$; the discussion and the expressions derived below can be easily generalized to the case of other OFQD's.

The contribution of the discrete bound-state level to eq. (4.21) can be computed using the expressions given in the Appendix. The result is shown in Fig. 1 for the forward case and Fig. 2 for a non-zero momentum transfer. Being taken by itself this contribution resembles the shape of $H(x, \xi, \Delta^2)$ obtained in the bag model [6].

To calculate the contribution of the Dirac continuum to eq. (4.21) we resort to an approximation which proved to be very successful in the computation of usual parton distributions, the so-called interpolation formula [12]. One first expresses the continuum contribution as a functional trace involving the quark propagator in the background pion field. The quark propagator can then be expanded in powers of the formal parameter $\partial U / (-\partial^2 + M^2)$, which becomes small in three limiting cases: *i*) low momenta, $|\partial U| \ll M$, *ii*) high momenta, $|\partial U| \gg M$, *iii*) any momenta but small pion fields, $|\log U| \ll 1$. One may therefore expect that this approximation has good accuracy also in the general case. As was shown in refs. [12, 14] for usual parton distributions this approximation preserves the positivity of the antiquark distributions and all sum rules; moreover, it gives results

very close to those obtained by exact numerical diagonalization of the Dirac hamiltonian and summation over the negative-energy levels.

To derive the interpolation formula for the isosinglet distribution $H(x, \xi, \Delta^2)$ (the expressions can easily be generalized to the case of isovector $E^{(3)}(x, \xi, \Delta^2)$) we proceed in analogy to the case of usual parton distributions [12] and rewrite the continuum contribution to eq. (4.21) as

$$\left[\sum_f H_f(x, \xi, \Delta^2) \right]_{\text{cont}} = \frac{N_c M_N}{2\pi T} \text{Im} \int dz^0 e^{iz^0 x M_N} \times \text{Sp} \left\{ (v_\mu \gamma^\mu) \exp[i\mathbf{\Delta} \cdot \mathbf{X} + z^0 (v_\mu \partial^\mu)] \frac{1}{[i\gamma^\mu \partial_\mu - M U^{\gamma_5} + i0]} \right\} - (U \rightarrow 1). \quad (4.25)$$

Here we have introduced a dimensionless light-like vector, $v_\mu = (1, 0, 0, 1)$, and T is the time interval which is canceled by a corresponding factor arising from the functional trace. We have written here explicitly the vacuum subtraction term. Expanding now in $\partial U / (-\partial^2 + M^2)$ and evaluating the the functional trace in momentum space one obtains in leading order:

$$\begin{aligned} & \left[\sum_f H_f(x, \xi, \Delta^2) \right]_{\text{cont}} \\ &= -2M_N N_c \text{Im} \int \frac{d^3 k}{(2\pi)^3} \int \frac{d^4 p}{(2\pi)^4} \delta \left[\left(x - \frac{\xi}{2}\right) M_N - v \cdot p \right] \\ & \quad \times \frac{M(p^2)}{(p^2 - M_0^2 + i0)} \frac{M((p-k)^2)}{(p-k)^2 - M_0^2 + i0} (k \cdot v) \text{Tr}_{\text{fl.}} \left\{ \tilde{U}(\mathbf{k} - \mathbf{\Delta}) [\tilde{U}(\mathbf{k})]^+ \right\} \\ & \quad + \left(\xi \rightarrow -\xi, \quad \mathbf{\Delta} \rightarrow -\mathbf{\Delta} \right), \end{aligned} \quad (4.26)$$

where the Fourier transform of the soliton field is defined as

$$\tilde{U}(\mathbf{k}) \equiv \int d^3 \mathbf{x} e^{-i\mathbf{k} \cdot \mathbf{x}} [U(\mathbf{x}) - 1]. \quad (4.27)$$

In eq. (4.26) we have re-instated the momentum dependence of the constituent quark mass, $M(p^2)$, which cuts the loop momentum p and thus regularizes the UV divergence; by M_0 we denote the value of the mass at zero momentum, $M(0)$. We have neglected in eq. (4.26) the momentum dependence of the quark masses appearing in the denominators; the masses standing in the denominators do not play the role of an UV regulator and their momentum dependence is not essential.

In ref.[12] the continuum contribution to the quark distribution functions was computed by regularizing the loop integrals with a relativistic Pauli-Villars cutoff. One may argue that this regularization mimics the effect of the momentum dependence of the constituent quark mass. [We shall soon see under which conditions this assumption is valid.] Let us evaluate the continuum contribution to the OFQD, eq. (4.26), also with a Pauli-Villars cutoff, neglecting the momentum dependence of the masses in the numerator. One

obtains

$$\begin{aligned}
\left[\sum_f H_f(x, \xi, \Delta^2) \right]_{\text{cont}} &= \frac{N_c M_N M_0^2}{2\pi} \text{sign} \left(x - \frac{\xi}{2} \right) \\
&\times \int \frac{d^3 k}{(2\pi)^3} \theta \left\{ - \left(x - \frac{\xi}{2} \right) M_N \left[\left(x - \frac{\xi}{2} \right) M_N - k^3 \right] \right\} \text{Re Tr}_{fl} \left\{ \tilde{U}(\mathbf{k} - \mathbf{\Delta}) [\tilde{U}(\mathbf{k})]^\dagger \right\} \\
&\times \int \frac{d^2 p_\perp}{(2\pi)^2} \frac{1}{|p_\perp|^2 + M_0^2 - \frac{|\mathbf{k}|^2}{(k^3)^2} \left(x - \frac{\xi}{2} \right) M_N \left[\left(x - \frac{\xi}{2} \right) M_N - k^3 \right]} \\
&+ \left(\xi \rightarrow -\xi, \mathbf{\Delta} \rightarrow -\mathbf{\Delta} \right), \tag{4.28}
\end{aligned}$$

where the last integral over transverse momenta is supposed to be regularized by the Pauli–Villars method, *i.e.*, by subtracting the equivalent integral with M replaced by the regulator mass, M_{PV} ; see [12] for details. [Here θ denotes the step function.] Eq. (4.28) has the remarkable property of being discontinuous at $|x| = \xi/2$. Such behaviour would lead immediately to a violation of the factorization theorems for, say, deeply virtual Compton scattering (DVCS) processes² [3], since the expression for the DVCS amplitude contains a factor

$$\text{Re} \int_{-1}^1 dx \left(\frac{1}{x - \xi/2 + i0} + \frac{1}{x + \xi/2 + i0} \right) \xi H(x, \xi, \Delta^2), \tag{4.29}$$

which would be logarithmically divergent if $H(x, \xi, \Delta^2)$ were discontinuous at $|x| = \xi/2$. However, this conclusion is premature: the discontinuities of eq. (4.28) are artifacts of neglecting the momentum dependence of the constituent quark mass, as we shall now show.

Let us analyze the original loop integral over p in eq. (4.26). By inspection of the denominators it is easy to see that for x close to $\pm\xi/2$ the dominant contribution to the integral comes from the region where the virtuality in one of the quark propagators becomes large,

$$(p - k)^2 \sim \frac{M_0(p_\perp^2 + M_0^2)}{(|x| - \xi/2)M_N}. \tag{4.30}$$

However, in this region, due to the presence of the momentum–dependent mass $M((p-k)^2)$ in the numerator, the whole expression drops to zero. More precisely, one can see that for

$$|x| - \xi/2 \sim \frac{(M_0\rho)^2 M_0}{M_N}, \tag{4.31}$$

where $\rho \sim (600 \text{ MeV})^{-1}$ is the characteristic scale of momentum dependence of the quark mass (the average instanton size), the integral over p_\perp is cut already at $p_\perp^2 \sim M_0^2$, whereas

²We are grateful to A.V. Radyushkin for discussion of this point

with a momentum-independent mass it would always be cut at $p_{\perp}^2 \sim 1/\rho^2$, see eq. (4.28). This analysis shows that the momentum dependence of the constituent mass *can not* be neglected for x in region eq. (4.31). Consequently, keeping the momentum dependence of the constituent quark mass, the discontinuities present in eq. (4.28) are smeared over an interval of order $(M_0\rho)^2/N_c$, so that the integral (4.29) is finite but it is still parametrically (and numerically) enhanced by a factor of $\log[(M_0\rho)^2/N_c]$; see the next section for numerical estimates. For values of x far from $\pm\xi/2$ the momentum dependence of the mass can be safely neglected and the simplified expression eq. (4.28) gives reliable approximation to eq.(4.26).

Let us also note that the points $x = \pm\xi/2$ divide the interval of the variable x ($-1 \leq x \leq 1$) in three regions: $x \leq -\xi/2$, where the function $H(x, \xi, \Delta^2)$ describes the antiquark distribution; $x \geq \xi/2$, where it corresponds to the quark distribution, and $-\xi \leq x \leq \xi/2$, where $H(x, \xi, \Delta^2)$ resembles a meson wave function. It is therefore natural that the functions $H(x, \xi, \Delta^2)$ has crossovers at $|x| = \xi/2$. This feature is remarkably reproduced in our model owing to the Dirac continuum contribution. We note that in the forward limit, $\Delta \rightarrow 0$, this crossover corresponds to the fact that *both* the quark and antiquark distributions are *positive*; hence the universal function $q(x)$ (which describes the quark distribution at $x \geq 0$ and *minus* the antiquark distribution at $x \leq 0$) evidently must exhibit a crossover at $x = 0$.

5 Numerical results and discussion

We have calculated numerically the isosinglet distribution $H(x, \xi, \Delta^2)$; the analogous calculations for other OFQD's can be done along the same lines. Our main purpose here is to discuss qualitative behaviour of the OFQD's; to this end it is sufficient to consider $H(x, \xi, \Delta^2)$. A comprehensive study of the other distributions will be given elsewhere.

For the numerical calculations we shall use the variational estimate of the soliton profile, eq.(eq. (3.13)), of ref.[10] ($M_0 = 350$ MeV),

$$P(r) = -2 \arctan\left(\frac{r_0^2}{r^2}\right), \quad r_0 \approx 1.0/M_0, \quad M_N \approx 1170 \text{ MeV}, \quad (5.32)$$

which has been used in the calculation of usual parton distributions in refs.[12, 14]. Furthermore, we approximate the momentum-dependent mass predicted by the instanton model of the QCD vacuum [19] by the simple form

$$M(-p^2) = \frac{M_0\Lambda^6}{(\Lambda^2 + p^2)^3}, \quad (5.33)$$

where the parameter Λ is related to the averaged instanton size, ρ , by $\Lambda = 6^{1/3}\rho^{-1}$. This form reproduces the asymptotic behaviour of $M(p^2)$ at large euclidean p^2 obtained in the instanton vacuum,

$$M(-p^2) \sim \frac{36M_0}{\rho^6 p^6} \quad (p^2 \rightarrow \infty).$$

We have explored also other forms of the momentum dependence of the mass and found that numerically the results are very close to each other.

We estimate the Dirac continuum contribution to $H(x, \xi, \Delta^2)$ using the interpolation formula, eq. (4.26), which gives a reliable approximation preserving all qualitative features of the continuum contribution. The contribution of the discrete level is calculated using eq. (A.5).

First we compute $H(x, \xi, \Delta^2)$ in the forward limit, $\Delta \rightarrow 0$, where it coincides with the usual quark and antiquark distributions. The result is shown in Fig. 1, where we plot separately the contributions of the discrete level and that of Dirac continuum (computed from the interpolation formula), as well as their sum. It should be emphasized that the distribution of *antiquarks* arising from the discrete level (see eq. (A.5)) is definitely negative and sizeable.³ Positivity of the parton distributions is restored only when one includes the contribution of the Dirac continuum. The full result for the function $H(x, 0, 0)$ (consisting of the level and continuum contributions) exhibits strong crossover at $x = 0$, corresponding to the fact that *both* the quark and antiquark distributions are positive. The crossover occurs in an x -interval of order $|x| < \sim 0.05$; we shall see that this remains so also for the off-forward case. To illustrate this we show in Fig. 2 the distribution $H(x, \xi, \Delta^2)$ as a function of x , for $\xi = 0.3$ and $\Delta_T^2 \equiv -\Delta^2 - \xi^2 M_N^2 = 0$. Again we have plotted separately the contributions of the discrete level and the Dirac continuum (according to the interpolation formula), as well as their sum. We see that the discrete level contribution is a smooth function which does not “know” about the points $x = \pm\xi/2$. This kind of behaviour has been assumed in all model approaches to OFQD’s, *e.g.* in the bag model calculations [6]. However the contribution of the Dirac continuum changes drastically the picture: the function $H(x, \xi, \Delta^2)$ shows now a fast crossover around the points $x = \pm\xi/2$. The interval of x over which this crossover occurs is of the order of ~ 0.05 , as in the forward case (see Fig. 1).

The fast crossover of $H(x, \xi, \Delta^2)$ at $x = \pm\xi/2$. may have physical implications. For example, it may lead to the considerable enhancement of the DVCS amplitude, because the crossover occurs exactly at the points where the integral eq. (4.29) entering the DVCS amplitude has singularities. Numerically, at $\xi = 0.3$ and $\Delta_T^2 = 0$ the contribution of the Dirac continuum to the integral (4.29) is 5.1 (almost the whole integral is collected in small vicinity of point $x = \pm\xi/2$), while the corresponding contribution of the discrete level is 3.2. We thus see that the crossover in $H(x, \xi, \Delta)$ contributes more than 60% to the integral (4.29) and may thus considerably increase the DVCS cross section.

In order to illustrate the dependence of $H(x, \xi, \Delta^2)$ on ξ and Δ^2 we plot this function for a fixed momentum transfer of $\Delta^2 = -0.5 \text{ GeV}^2$ for various values of ξ (see Fig. 3), and for fixed $\xi = 0.3$ and various values of momentum transfer (see Fig. 4).

In the large N_c limit the nucleon is heavy, so the OFPD’s do not automatically go to zero at $x = 1$; see the discussion in [12]. However, at $x \gg 1/N_c$ the distributions behave as $\sim \exp(-\text{const} \cdot N_c x)$. Numerically, even for $N_c = 3$ all distributions computed are very small at $x \approx 1$.

³In the extreme case of a very strongly bound discrete level when it approaches the lower continuum, this level would not produce quarks at all – only antiquarks, but with a negative sign!

6 Conclusions

In this paper we have investigated the off-forward quark distribution (OFQD's) functions in the nucleon in the large- N_c limit. At large N_c the nucleon can be viewed as a heavy semiclassical body whose N_c “valence” quarks are bound by a self-consistent pion field. The energy of the pion field is given by the effective chiral lagrangian and coincides with the aggregate energy of the Dirac sea of quarks (the free continuum subtracted). To compute the quark and antiquark distributions (forward and off-forward) one must sum the contributions from the discrete level and from the (distorted) negative-energy Dirac continuum.

We have found that the flavour singlet off-forward distribution $H(x, \xi, \Delta^2)$ exhibits a qualitatively new behaviour due to the contribution of the Dirac continuum: The function shows fast crossovers around the points $x = \pm\xi/2$. Our numerical estimates indicate that this crossover could lead to a considerable enhancement of the deeply virtual Compton scattering cross section.

In the crossover regions the behavior of the OFQD's is essentially determined by the momentum dependence of the constituent quark mass generated in the dynamical breaking of chiral symmetry. In particular, the region in x over which the crossover takes place is proportional to $(M_0\rho)^2/N_c$, where ρ is the characteristic momentum scale at which the dynamical quark mass drops to zero — the average instanton size. Thus, the enhancement of the deeply virtual Compton scattering cross section is governed by the small parameter intrinsic to the instanton model of the QCD vacuum, the packing fraction of the instanton medium, $(M_0\rho)^2 \propto (\rho/R)^4$.

The OFQD calculated here in the chiral quark-soliton model refers to a low normalization point of order the UV cutoff intrinsic in this model, $\rho^{-1} \approx 600$ MeV. To obtain the OFQD's at higher normalization points one has to evolve the “primordial” distributions using the evolution equations derived in refs.[3, 4, 8, 7]. With regard to the description of experiments it would be extremely interesting to study to what extent the crossovers at $x = \pm\xi/2$ persist when evolved to higher normalization points.

Acknowledgements

We are grateful to L. Mankiewicz, M. Strikman and A. Radyushkin for inspiring conversations. This work has been supported in part by the RFBR (Moscow), Deutsche Forschungsgemeinschaft (Bonn) and by COSY (Jülich). The Russian participants acknowledge the hospitality of Bochum University. M.V.P. is being supported by the A.v.Humboldt Foundation.

A Bound-state level contribution to $H(x, \xi, \Delta^2)$

We present here the contributions of the discrete bound-state level to the singlet $H(x, \xi, \Delta^2)$. The bound-state level occurs in the grand spin $K = 0$ and parity $\Pi = +$ sector of the Dirac hamiltonian (3.10). In that sector the eigenvalue equation takes the form:

$$\begin{pmatrix} M \cos P(r) & -\frac{\partial}{\partial r} - \frac{2}{r} - M \sin P(r) \\ \frac{\partial}{\partial r} - M \sin P(r) & -M \cos P(r) \end{pmatrix} \begin{pmatrix} h_0(r) \\ j_1(r) \end{pmatrix} = E_{\text{lev}} \begin{pmatrix} h_0(r) \\ j_1(r) \end{pmatrix} \quad (\text{A.1})$$

We assume that the radial wave functions are normalized by the condition

$$\int_0^\infty dr r^2 [h_0^2(r) + j_1^2(r)] = 1. \quad (\text{A.2})$$

We introduce the Fourier transforms of the radial wave functions,

$$h(k) = \int_0^\infty dr r^2 h_0(r) R_{k0}(r), \quad j(k) = \int_0^\infty dr r^2 j_1(r) R_{k1}(r), \quad (\text{A.3})$$

where

$$R_{kl}(r) = \sqrt{\frac{k}{r}} J_{l+\frac{1}{2}}(kr) = (-1)^l \sqrt{\frac{2}{\pi}} \frac{r^l}{k^l} \left(\frac{1}{r} \frac{d}{dr} \right)^l \frac{\sin kr}{r}. \quad (\text{A.4})$$

The bound-state level contribution to the singlet $H(x, \xi, \Delta^2)$ distribution function can be simply obtained from the general eq. (4.21). We get:

$$\begin{aligned} \sum_f H_f(x, \xi, \Delta^2)_{\text{lev}} &= 2\pi N_c M_N \int \frac{d^2 \mathbf{k}_\perp}{(2\pi)^2} \frac{1}{kk'} \left\{ h(k)h(k') \right. \\ &+ j(k)j(k') \frac{\mathbf{k}_\perp \cdot (\mathbf{k}_\perp + \boldsymbol{\Delta}_\perp) + (xM_N - E_{\text{lev}})^2 - \frac{1}{4}\xi^2 M_N^2}{kk'} \\ &\left. - h(k)j(k') \frac{xM_N - E_{\text{lev}} + \frac{1}{2}\xi M_N}{k} - h(k')j(k) \frac{xM_N - E_{\text{lev}} - \frac{1}{2}\xi M_N}{k'} \right\}, \end{aligned} \quad (\text{A.5})$$

where

$$k = \sqrt{\mathbf{k}_\perp^2 + \left((x + \frac{1}{2}\xi)M_N - E_{\text{lev}} \right)^2} \quad (\text{A.6})$$

$$k' = \sqrt{(\mathbf{k}_\perp + \boldsymbol{\Delta}_\perp)^2 + \left[(x - \frac{1}{2}\xi)M_N - E_{\text{lev}} \right]^2}. \quad (\text{A.7})$$

Note that the r.h.s. of eq. (A.5) is positive in the forward limit ($\Delta \rightarrow 0$) for all values of x , in particular at $x < 0$ where eq. (A.5) determines in fact the antiquark distribution. Since $\bar{q}(x) = -H(-x, 0, 0)$, it means that eq. (A.5) gives a *negative* distribution of antiquarks at $x > 0$. At the same time it is easy to check by integrating over x eq. (A.5) that the baryon number sum rule is fully saturated by the discrete-level contribution only.

References

- [1] X. Ji, Phys. Rev. Lett. **78** (1997) 610.
- [2] A. V. Radyushkin, Phys. Lett. **B380** (1996) 417.
- [3] X. Ji, Phys. Rev. **D55** (1997) 7114.
- [4] A.V. Radyushkin, Phys. Lett. **B285** (1996) 333.
- [5] J. Collins, L. Frankfurt, and M. Strikman, Phys. Rev. **D56** (1997) 2982.
- [6] X. Ji, and W. Melnitchouk, and X. Song, *A study of off-forward parton distributions*, DOE/ER/40762-114, Archive [hep-ph/9702379](#), to be published in Phys. Rev. **D**.
- [7] A.V. Radyushkin, *Nonforward parton distributions*, JLAB-THY-97-10, Archive [hep-ph/9704207](#), to be published in Phys. Rev. **D**.
- [8] L. Frankfurt, A. Freund, V. Guzey, and M. Strikman, *Nondiagonal parton distribution in the leading logarithmic approximation*, e-Print Archive: [hep-ph/9703449](#), J. Blümlein, B. Geyer, and D. Robaschik, Phys. Lett. **406B** (1997) 161; I.I. Balitskii, and A.V. Radyushkin, *Light ray evolution equations and leading twist parton helicity dependent nonforward distributions*, JLAB-THY-97-21, e-Print Archive: [hep-ph/9706410](#); A.V. Belitskii, D. Mueller, *Predictions from conformal algebra for the deeply virtual Compton scattering*, NTZ-23-97, e-Print Archive: [hep-ph/9709379](#).
- [9] Chr. V. Christov *et al.*, Prog. Part. Nucl. Phys. **37** (1996) 91.
- [10] D.I. Diakonov, Yu.V. Petrov and P.V. Pobylitsa, Nucl. Phys. **B306** (1988) 809
- [11] D. Diakonov, M. Polyakov, and C. Weiss, Nucl. Phys. **B461** (1996) 539.
- [12] D. Diakonov, V. Petrov, P. Pobylitsa, M. Polyakov, and C. Weiss, Nucl. Phys. **B480** (1996) 341
- [13] P.V. Pobylitsa, and M.V. Polyakov, Phys. Lett. **389B** (1996) 350.
- [14] D.I. Diakonov, V. Yu. Petrov, P.V. Pobylitsa, M.V. Polyakov and C. Weiss, Phys. Rev. **D 56** (1997) 4069.
- [15] E. Witten, Nucl. Phys. **B223** (1983) 433.
- [16] G. Adkins, C. Nappi and E. Witten, Nucl. Phys. **B228** (1983) 552.
- [17] D. Diakonov and M. Eides, Sov. Phys. JETP Lett. **38** (1983) 433.
- [18] A. Dhar, R. Shankar and S. Wadia, Phys. Rev. **D31** (1984) 3256.
- [19] D. Diakonov and V. Petrov, Nucl. Phys. **B272** (1986) 457; LNPI preprint LNPI-1153 (1986), published (in Russian) in: Hadron matter under extreme conditions, Naukova Dumka, Kiev (1986), p.192.

- [20] D.I.Diakonov and V.Yu.Petrov, Nucl. Phys. **B203** (1984) 259.
- [21] S. Kahana, G. Ripka and V. Soni, Nucl. Phys. **A415** (1984) 351;
S. Kahana and G. Ripka, Nucl. Phys. **A429** (1984) 462.
- [22] M.S. Birse and M.K. Banerjee, Phys. Lett. **B136** (1984) 284.
- [23] C. Christov, A.Z. Gorski, K. Goeke, and P.V. Pobylitsa, Nucl. Phys. **A592** (1995) 513.
- [24] H. Weigel, L. Gamberg, H. Reinhardt, Phys. Lett. **B399** (1997) 287.

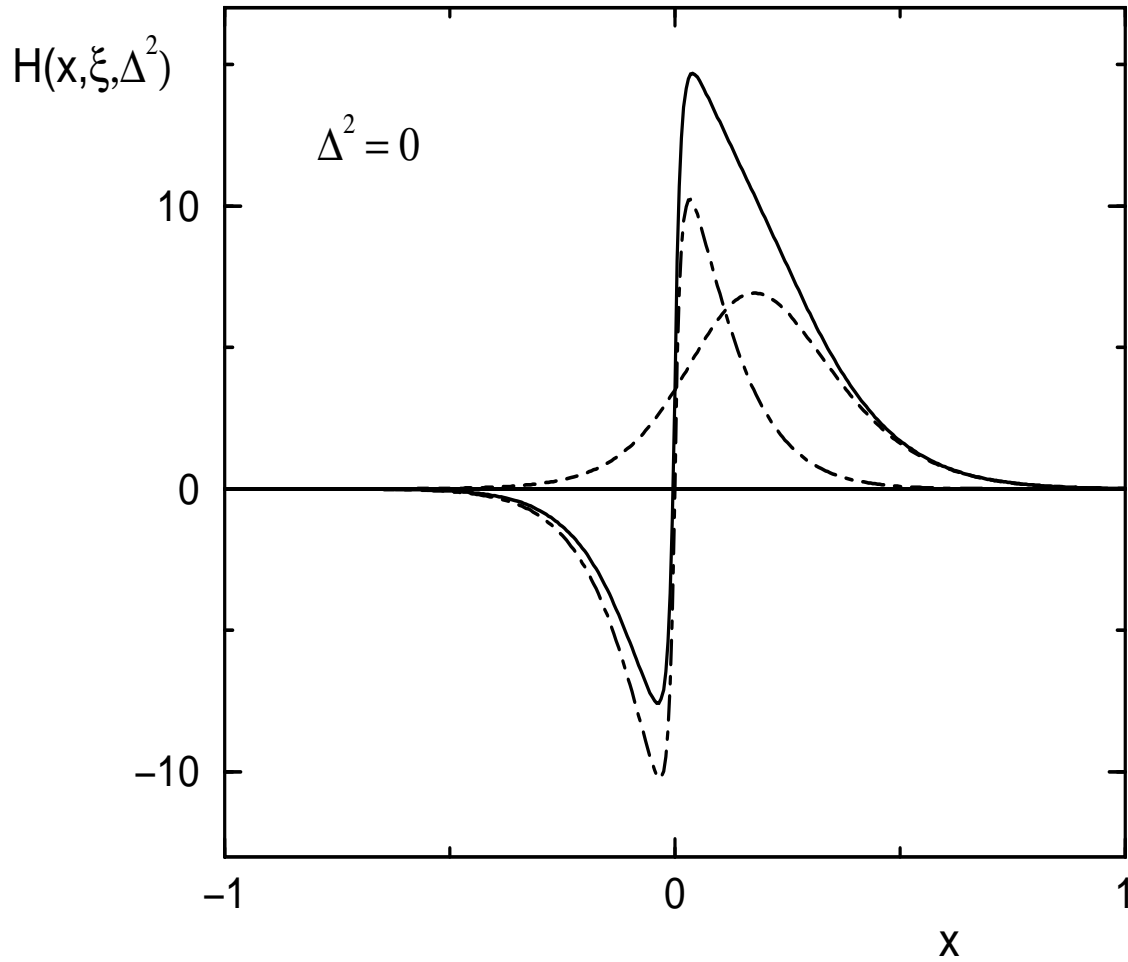


Figure 1: The isosinglet distribution $H(x, \xi, \Delta^2)$ in the forward limit, $\Delta = 0$. *Dashed line*: contribution from the discrete level. *Dashed-dotted line*: contribution from the Dirac continuum according to the interpolation formula, eq. (4.26). *Solid line*: total distribution (sum of the dashed and dashed-dotted curves).

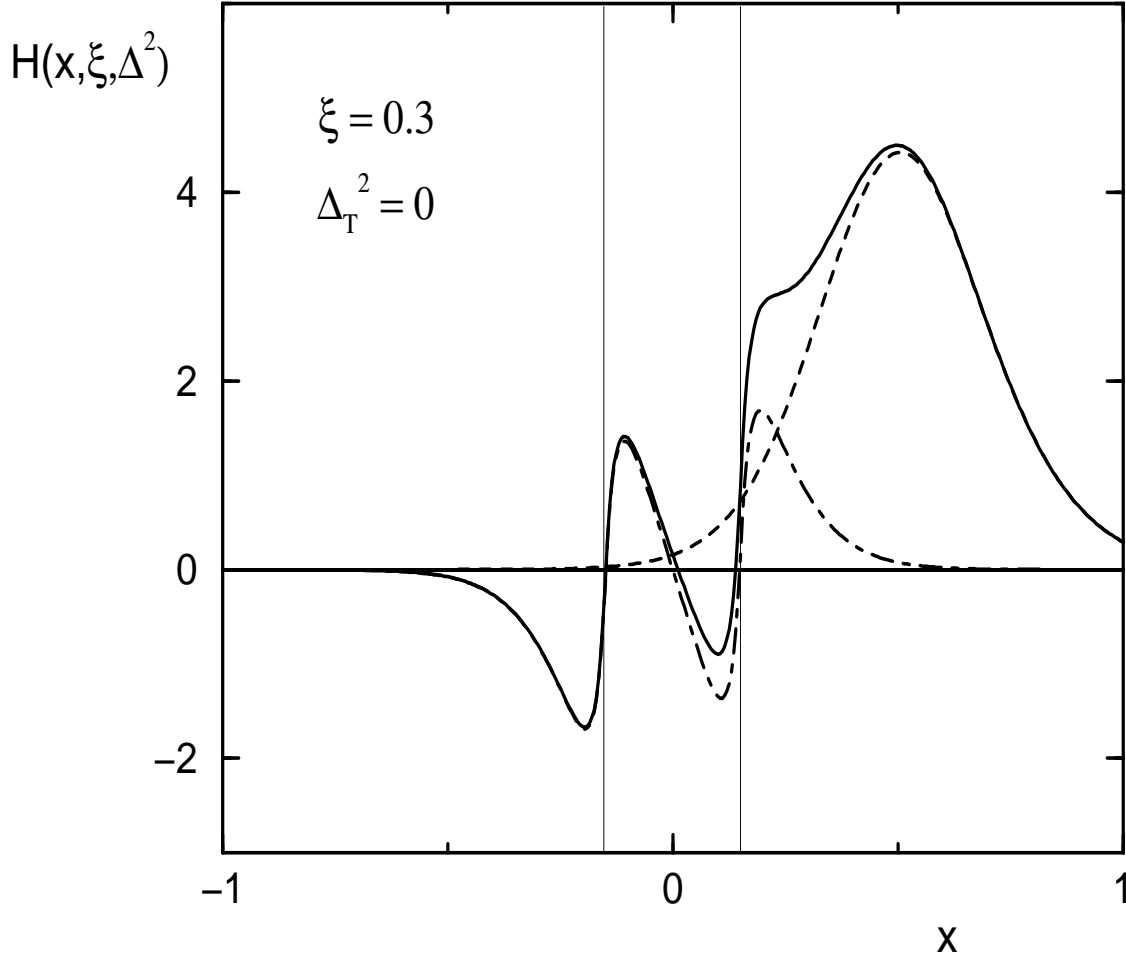


Figure 2: The isosinglet distribution $H(x, \xi, \Delta^2)$ for $\Delta_T^2 = 0$ ($\Delta_T^2 \equiv -\Delta^2 - \xi^2 M_N^2$) and $\xi = 0.3$. *Dashed line*: contribution from the discrete level. *Dashed-dotted line*: contribution from the Dirac continuum according to the interpolation formula, eq. (4.26). *Solid line*: the total distribution (sum of the dashed and dashed-dotted curves). The vertical lines mark the crossover points $x = \pm\xi/2$.

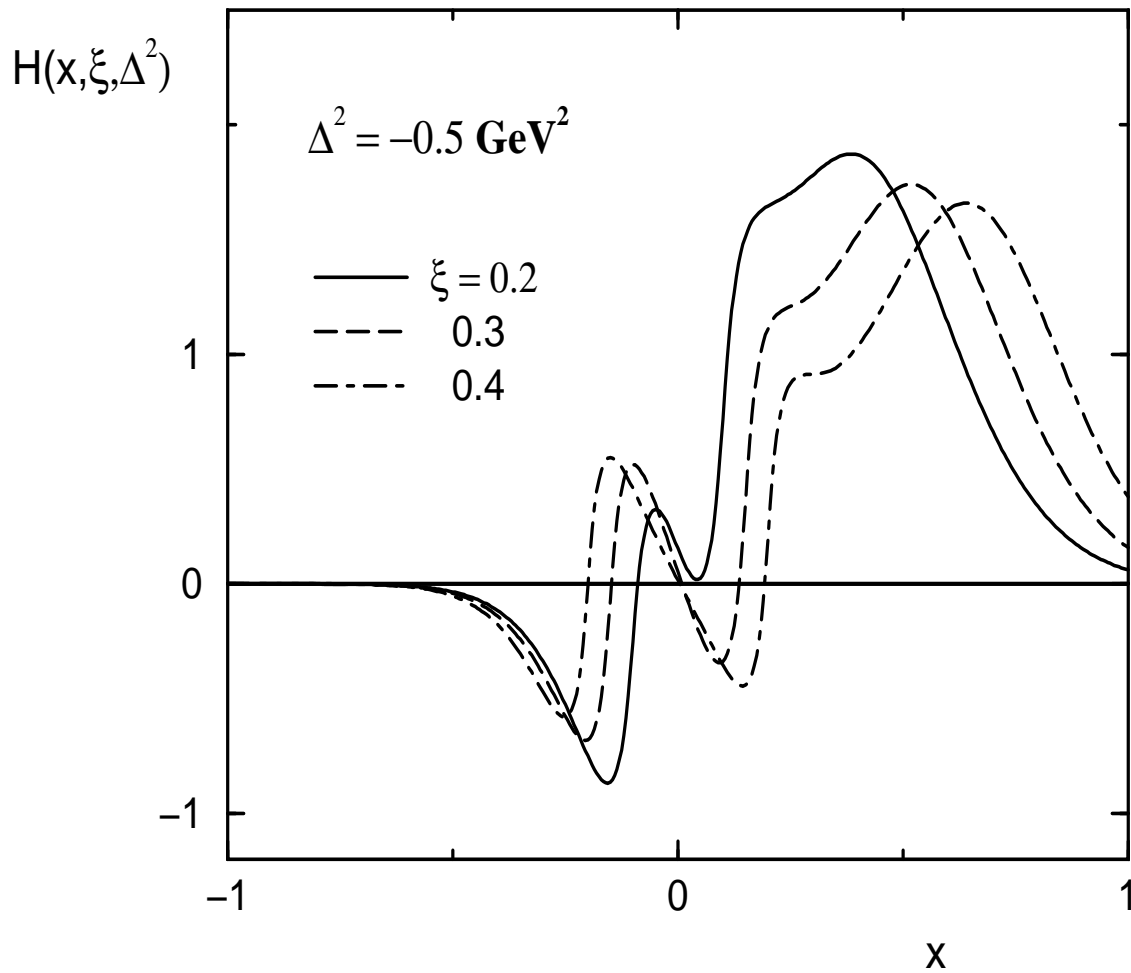


Figure 3: The isosinglet distribution $H(x, \xi, \Delta^2)$ (total result) for fixed $\Delta^2 = -0.5 \text{ GeV}^2$ and various values of ξ .

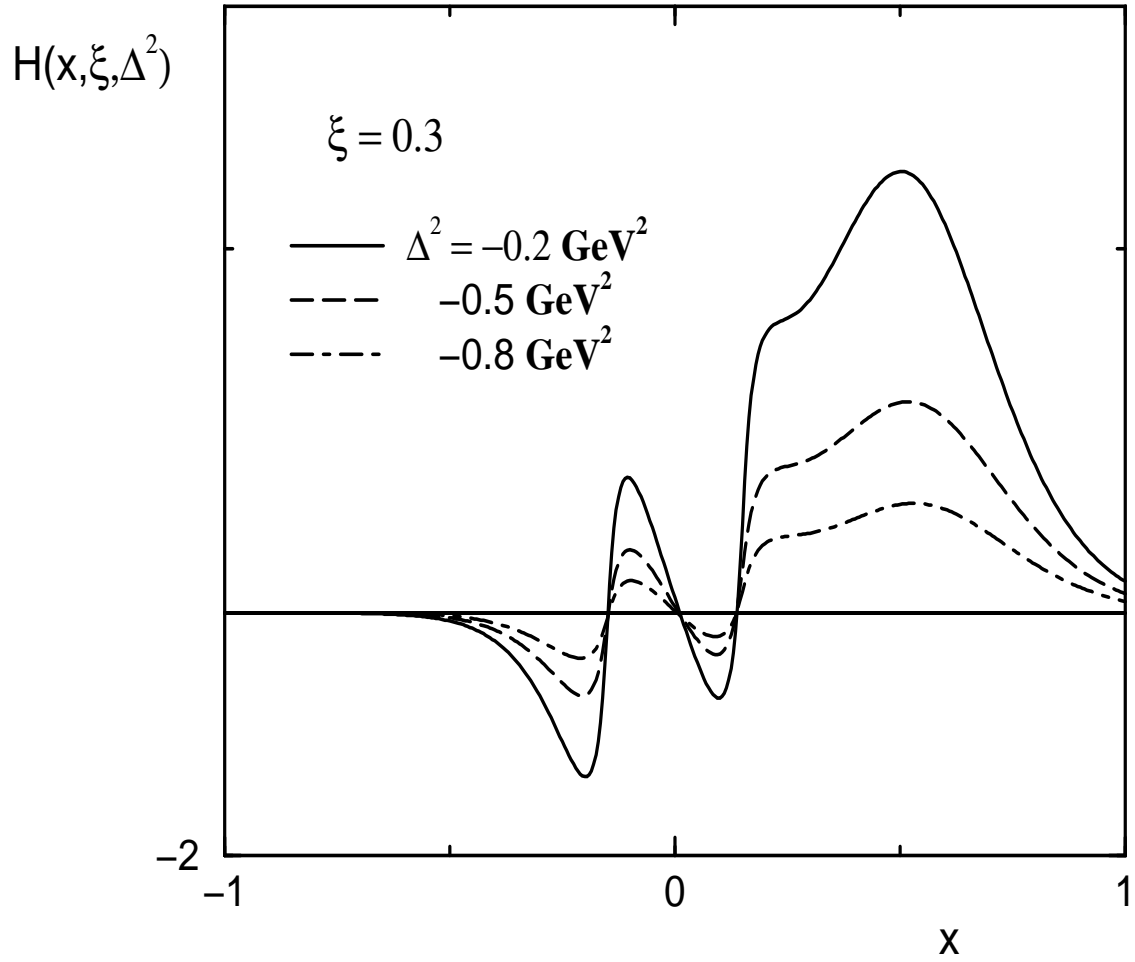


Figure 4: The isosinglet distribution $H(x, \xi, \Delta^2)$ (total result) for fixed $\xi = 0.3$ and various values of Δ^2 .